

Advanced imaging of hybrid acquisition data: Exploring new frontiers

Sylvain Masclet^{1*}, Fang Wang¹, Guillaume Henin¹, Loic Janot¹, Olivier Hermant¹, Hao Jiang¹, Nicolas Salaun¹, David Le Meur¹ and Daniela Donno¹ illustrate how the leveraging of sparse node data through an interferometry approach and the use of elastic FWI can enhance streamer seismic imaging.

Introduction

In recent years, two predominant acquisition trends have emerged: multi-source dense streamer acquisition, ideal for shallow targets requiring high-resolution imaging, and ocean bottom node (OBN) acquisition, initially designed for complex sub-salt imaging. Dense streamer acquisitions enhance subsurface image resolution, particularly in regions with challenging conditions such as very hard seafloor and fast shallow sediments. This improvement is achieved by towing streamers closer to wide-towed sources (Long et al., 2017) or deploying source-over-spread technology (Lie et al., 2018). OBN data, featuring rich low-frequency signals, full-azimuth coverage, and long-offset illumination, offer significant advantages for enhancing seismic velocity models and imaging. However, the operational cost of using dense nodes generally limits their deployment to known reservoirs with restricted shot coverage and maximum offset. Consequently, during the exploration phase, narrow-azimuth towed-streamer (NATS) acquisitions are often preferred. However, NATS data can lead to inadequate imaging of complex targets, increasing uncertainty and risk in prospect estimation.

Increasing node spacing, even up to 1 km intervals (sparse nodes), has emerged as a potential solution to economically expand the imaged area while leveraging the benefits of node data for velocity model-building with full-waveform inversion (FWI) (Dellinger et al., 2017). The extended offsets allow for deeper diving-wave penetration, a crucial aspect of FWI updates. The full-azimuth coverage enhances inversion constraints, benefiting from diverse travelpath angles, while rich low-frequency content compensates for starting model inaccuracies (Michell et al., 2017; Shen et al., 2017). While node sparsity does not affect low-frequency FWI for model building, imaging with nodes at 1 km spacing may still face challenges in providing the necessary resolution for reservoir-level details. To mitigate this limitation, a hybrid acquisition approach combining sparse nodes and dense streamers has emerged as a cost-effective solution for large exploration areas. Such multi-input data acquisitions require innovative processing and imaging techniques to fully exploit their potential.

From the challenging areas of the Nordkapp Basin in the Barents Sea to those of the Northern North Sea, this paper illustrates

how the leveraging of sparse node data through an interferometry approach and the use of elastic FWI can enhance streamer seismic imaging. As a result, building a high-resolution velocity model with an accurate low-frequency background reduces exploration risk and pushes the limits of imaging technologies one step further forward.

Imaging the salt domes in the Nordkapp basin

Geology and challenges

The Nordkapp Basin, located in the southern part of the Barents Sea, is a large, underexplored salt basin with a proven petroleum system containing mature Triassic source rocks with expected hydrocarbon traps located at a depth of approximately 3 km. Salt diapirism is prolific with diapirs penetrating all the way up to the seafloor (Figure 1). The imaging challenges of this exploration region are also related to the huge Tertiary uplift which brings high-velocity strata up to very shallow depths. This creates very strong multiple energy and also reduces the incidence angle in the very shallow section.

Based on the geologic understanding of the Nordkapp Basin and the corresponding geophysical challenges, a hybrid blended acquisition was performed, combining 18-cable streamer data with sources located in front of and above the streamers and sparse OBN (Dhelie et al., 2021). With such a design, high-

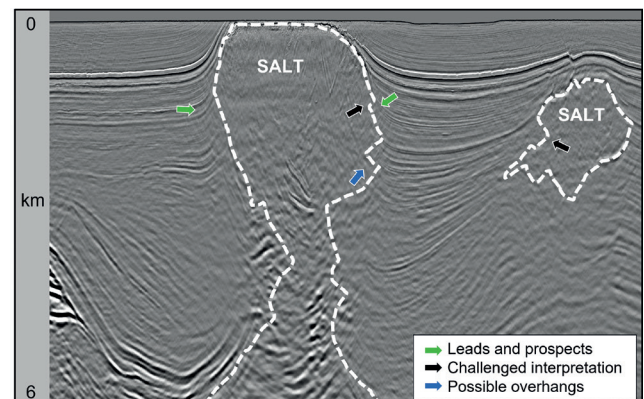


Figure 1 3D seismic section across the Nordkapp Basin central area, showing the distinct salt diapirism.

¹CGG

* Corresponding author, E-mail: sylvain.mascllet@cgg.com

DOI: 10.3997/1365-2397.fb2023105

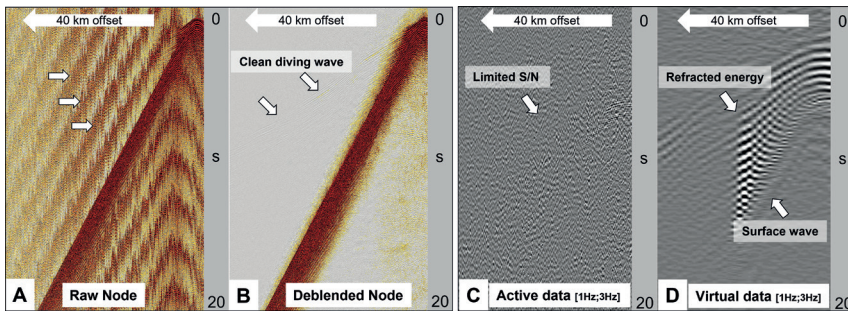


Figure 2 Raw node gathers before a) and after b) a comprehensive deblending workflow allowing recovery of diving waves above 3 Hz. Active c) and virtual d) seismic gather at low frequency (1-3 Hz); while the active node exhibits residual blended energy, refracted and surface waves are visible on the virtual gather.

resolution and high-fidelity imaging can be achieved by combining the dense streamer data with the wide-azimuth and long-offset (up to 40 km) receiver gathers provided by the OBN records. As a result of the use of a very sparse node carpet with 1200 m between nodes, a large-scale OBN acquisition covering an exploration area of 3700 km² was economically viable.

Ultra-low frequency data reconstruction by interferometry

To achieve a high-resolution subsurface sampling within a limited amount of time, a dense shooting carpet was required. With seven sources shooting almost simultaneously, and one shot-point every 2.5 seconds on average, severe blending noise appears on the recorded OBN data, affecting its signal-to-noise ratio. To use long-offset refraction energy for FWI, we needed to de-blend the data down to a 20-second interval (Figure 2a). Achieving this required the removal of more than 12 orders of blending noise, which we accomplished through a node-by-node inversion-based deblending approach, revealing weak diving wave energy along the 40 km offset (Figure 2b). However, due to the small dithers (± 200 ms) used for blending noise randomisation, recovering low frequencies below 3 Hz through deblending was challenging, preventing FWI from starting below this frequency (Figure 2c). Conventional velocity modelling methods attempt to compensate for this by incorporating more accurate initial velocity models based on salt interpretation. But in such complex geology, even starting at 3 Hz, FWI may fall into local minima (cycle skipping) problems due to potential inaccuracies in the initial model. Fortunately, OBNs were continuously deployed on the water bottom for three months without redeployment. This continuous recording enabled interferometry to reconstruct ultra-low frequencies (Figure 2d). Interferometry uses continuous seismic data to create virtual

sources at receiver locations, a technique proven to be effective in Middle East land datasets (Le Meur et al., 2020) for velocity model building. By combining cross-correlations and temporal stacking, we generated virtual source gathers, capturing both active sources and environmental noise contributions. This approach allowed us to produce ultra-long offset sparse gathers with 1200 m spacing, effectively reconstructing surface and diving waves down to 0.5 Hz. Interferometry provides a solution for recovering low-frequency signals that conventional active data cannot capture.

The virtual gathers also captured ultra-low frequency surface waves with a minimum frequency of 0.3 Hz. Unlike active data, where picking of surface-wave dispersion curves can be challenging (Figure 3a), virtual shots enabled phase velocity picking from 0.4 Hz to 1 Hz for the surface waves and also from 1 Hz for the guided waves (Figure 3b). As the surface-wave frequency content reflects its penetration depth (Strobbia et al., 2011), we combined these dispersion curve picks with first-break data to perform multi-wave inversion (Bardainne, 2018) for updates of both P-wave (V_p) and S-wave (V_s) velocity in the shallow section down to 300 m in depth. Figure 3c shows the result of 200 Hz FWI of the top of salt (Espin et al., 2022), while Figure 3d displays V_p/V_s information at a shallow level through the top salt region, revealing the diapir's heterogeneous composition. Virtual data provides valuable information for geotechnical evaluation of subsurface layer consolidation and can serve as a starting point for creating an input V_s model for elastic FWI when well information is unavailable.

Full-waveform inversion using virtual and active seismic data

Using 991 nodes with virtual shots at node positions, interferometry-based virtual gathers offered offsets up to 40 km, allowing V_p

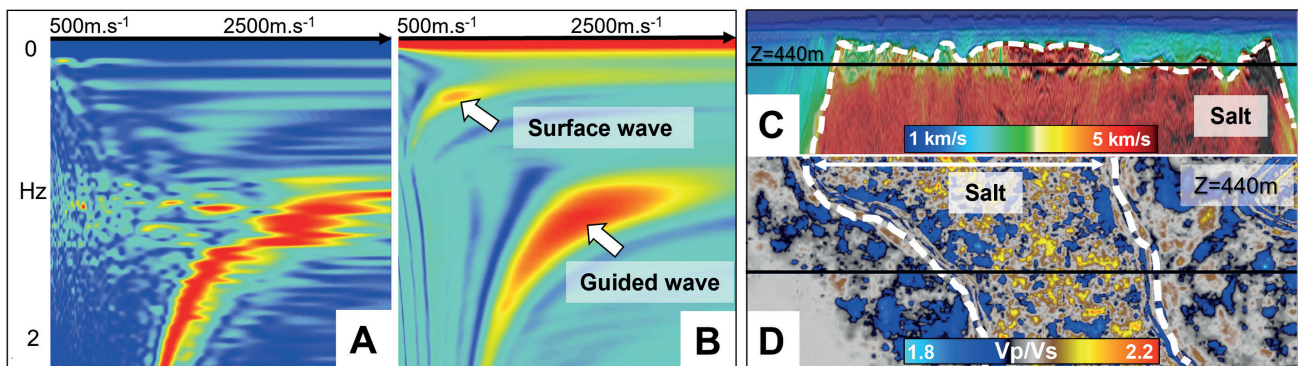


Figure 3 Dispersion panels for surface and guided waves in the case of active (a) and virtual gathers (b). V_p model obtained from 200 Hz Acoustic FWI (c) and inverted V_p/V_s at a shallow depth slice going through a salt diapir (d), which shows its heterogeneous composition.

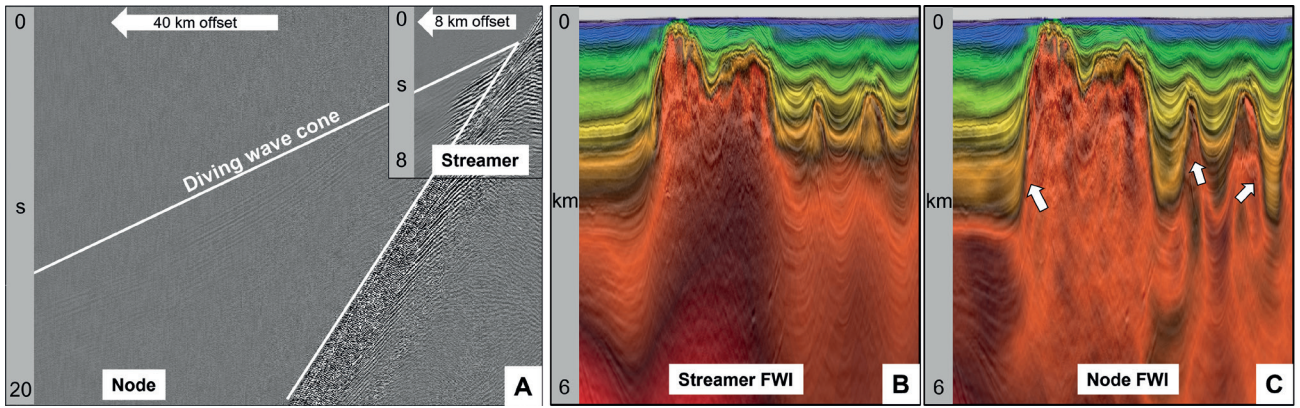


Figure 4 a) Ultra-long offset OBN gather after deblending. Comparison of migrated seismic overlaid with velocity models of a) streamer and b) node FWI.

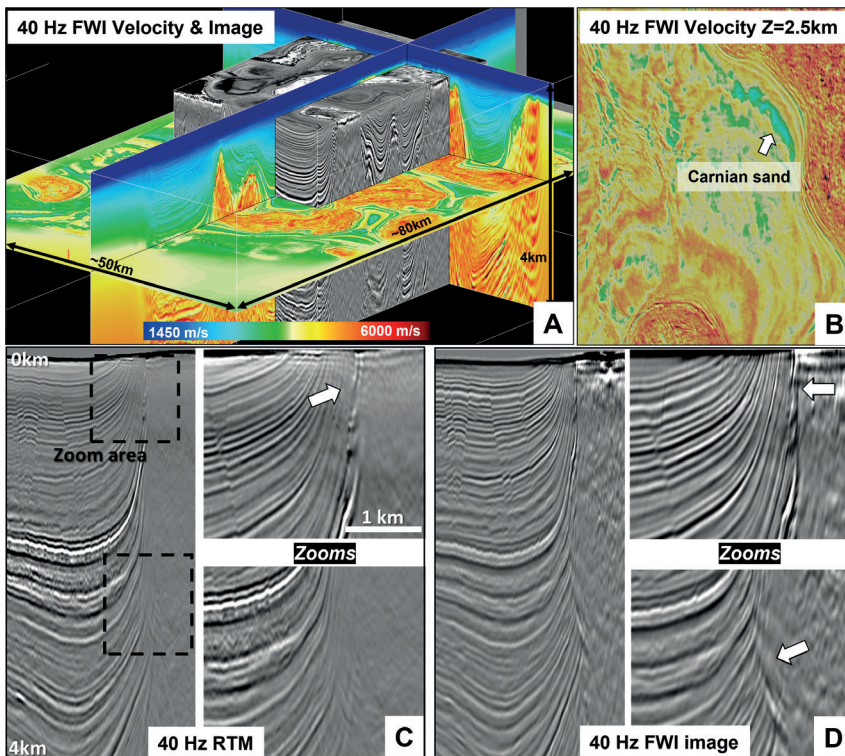


Figure 5 a) 3D view of 40 Hz FWI velocity model and FWI image over Nordkapp survey. b) Depth slice going through the target level, with the high-resolution model giving clear insight into the extent of the Carnian sands. Comparison of 40 Hz RTM stack image c) and 40 Hz FWI Image d) around the salt edges.

updates down to 6 km in depth. FWI using virtual data was run up to 3 Hz due to data sparsity at higher frequencies. Interferometry ensured FWI convergence starting at 1 Hz, even with complex salt structures. Active seismic nodes were then used for FWI above 3 Hz. After deblending, reflections and diving waves were effectively recovered at offsets up to 40 km and 20 s of record length (Figure 4a). Node data conveniently supplemented streamer data which are dense but limited in offset and diving-wave penetration depth. In the Nordkapp basin, where salt diapirs and high seismic velocities pose challenges, the FWI result obtained using only streamer data shows a limited depth update owing to the limited offset range (Figure 4b). Our new FWI approach, using both active and virtual node data, improved salt contour definition from low-frequency updates (Figure 4c) without the need for manual salt body interpretation. This method offers an alternative to ray-based tomography and reduces cycle skipping risks by starting at 1 Hz.

Moving to high-resolution full-waveform inversion and imaging

Recent advances in FWI (Zhang et al., 2018) enable us to fully leverage the full wavefield, including diving waves, reflections, and their multiples and ghosts. These components are especially valuable for high-frequency updates and enhance the velocity model details. By increasing the inversion frequency, we can reveal reservoir information that conventional seismic reflection methods cannot capture. To achieve the highest FWI resolution, we utilised all types of waves in the records, ensuring balanced illumination and avoiding migration artifacts and spatial sampling issues. Node gathers accurately captured the long-wavelength trend of the velocity model down to a 6 km depth. However, the lack of near offsets, related to the sparse node grid for the recorded primaries and multiples, prevented FWI updates with nodes above 10 Hz. For higher-frequency FWI, the streamer dataset, with its dense spatial sampling and

additional near-offset data, outperformed sparse OBN data, effectively addressing spatial aliasing issues at high frequencies for the shallower part of the velocity model. The high-frequency FWI utilised the entire records up to 40 Hz, making it possible to obtain model updates down to depths of 4 km, although this required substantial computational resources to cover the total volume of over 16,000 km³ (Figure 5a). The 40 Hz inversion already revealed clear details of the Carnian sand target (Figure 5b, white arrow) in the velocity model. For conventional imaging, we used the 10 Hz FWI update as the migration velocity model for running reverse-time migration (RTM) with streamer data, which delivered an accurate image of the salt bodies (Figure 5c). Our next step was to generate a FWI Image from the 40 Hz velocity model (Zhang et al., 2020). The FWI Image (Figure 5d) significantly enhanced imaging of the complex vertical salt wall's steep dips compared to RTM (Figure 5c) and provided better delineation of salt bodies, thanks to the least-squares process of the FWI engine and utilisation of the entire wavefield.

Unlocking new targets below the Base Cretaceous Unconformity (BCU) in the Northern North Sea: Fram and Oseberg surveys

Geology and challenges

Exploration in the Northern North Sea has a long history, with ongoing discoveries and evolving exploration models. Recent finds in the Upper Jurassic sands (Dugong in 2020, Echino Sør in 2019), just below the Base Cretaceous Unconformity (BCU), have underscored the need for precise structural mapping of fault traps and, consequently, more accurate velocity models down to the sub-BCU level. Challenges arise from high-velocity injectites in the shallow section, a limestone/carbonate sequence with high velocities covering the targeted lower velocity mudstone units, and extensively faulted Jurassic blocks (Figure 6b). These challenges become more significant because they typically occur at depths beyond the reach of diving waves for FWI when using streamer-based data with a maximum 8 km offset. In response to the growing focus on near-field exploration and the search for less obvious deeper targets in the Northern Viking Graben (NVG) region, two successive hybrid blended acquisitions were recently completed in 2021 and 2022 over the NVG area. In addition to

an existing north-south 3D seismic survey spanning 44,000 km² (blue polygon in Figure 6a), a blended hybrid acquisition was deployed. This approach combined an east-west oriented triple-source streamer survey with a 900 m x 900 m node grid. It provided a maximum offset of up to 24 km for the Fram survey (~50 km², white polygon) and up to 60 km for the Oseberg survey (~2,000 km², black polygon).

Exploiting diving waves below the BCU

In 2018 the Fram and Oseberg areas were initially imaged using the north-south streamer data. A velocity model was built with visco-acoustic FWI (Q-FWI; Xiao et al., 2018) and tomography, and the image was obtained with attenuation-compensating Kirchhoff pre-stack depth migration (Q-KPSDM) as shown in Figure 7b for the Fram survey and Figure 8c for the Oseberg survey. With a maximum offset of 8 km, streamer-only FWI provided reliable updates down to ~2 km depths, partially resolving velocity contrasts caused by injectites. However, reaching sub-BCU levels, from 2.5 km in Fram to 5 km in Oseberg, is beyond the streamer data's FWI capability. Tomography is needed for a deeper velocity update but is prone to inaccuracies due to multiples and the single-arrival assumption, leading to uncertain prospect interpretations. Sparse node data, with ultra-long offsets, is crucial for extending low-wavenumber FWI updates to sub-BCU levels (Lie et al., 2022). Diving-wave analysis using the 2018 legacy model shows that increasing the maximum offset from 8 km to 24 km in the Fram area deepens the diving wave penetration from 2 km to 4.5 km. A comparison between streamer-only and streamer and node diving wave FWI in the Oseberg area (Figures 8a and 8b) highlights the deep penetration of the longer offset, node-recorded, diving waves, capturing lateral velocity variations caused by complex sediment basins and faulted blocks. Starting with a smoothed 2018 legacy velocity model, we conducted acoustic FWI with an advanced time-lag cost function (A-FWI; Zhang et al., 2018) using only diving waves to obtain a reliable low-wavenumber update, essential for the higher-frequency model refinement.

In the Fram survey, the 6 Hz FWI using node data managed to capture the velocity inversion below the BCU and provides a good background velocity down to 4.5 km depth (Figure 7a).

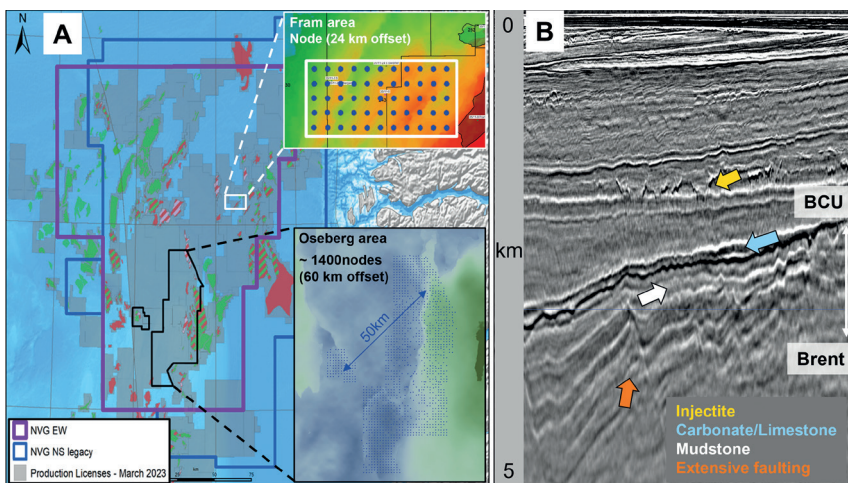


Figure 6 a) Location map showing legacy north-south and new east-west seismic data coverage, and sparse OBN layouts in the NVG area. b) 3D section across the Fram survey illustrating common geological features in the region and the associated geophysical challenges.

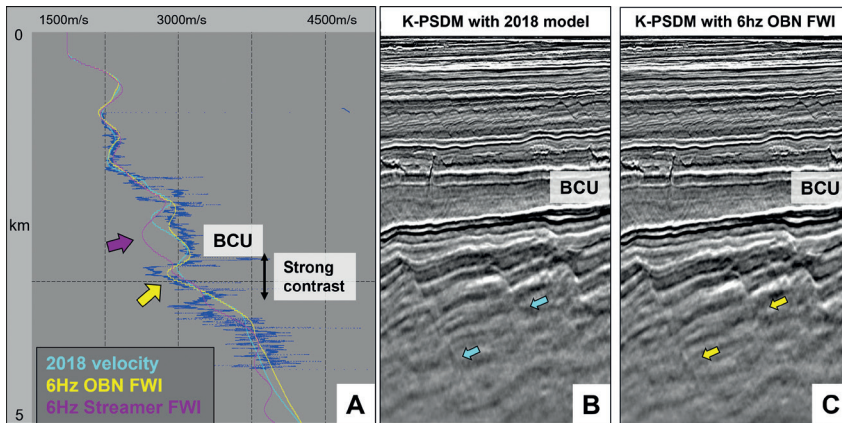


Figure 7 Fram survey: a) velocity profile at well location with sonic log (dark blue), 2018 legacy model (cyan), after 6 Hz A-FWI with streamer data (pink) and after 6 Hz A-FWI with node data (yellow). K-PSDM stack images using b) the 2018 legacy model and c) the 6 Hz A-FWI model with node data.

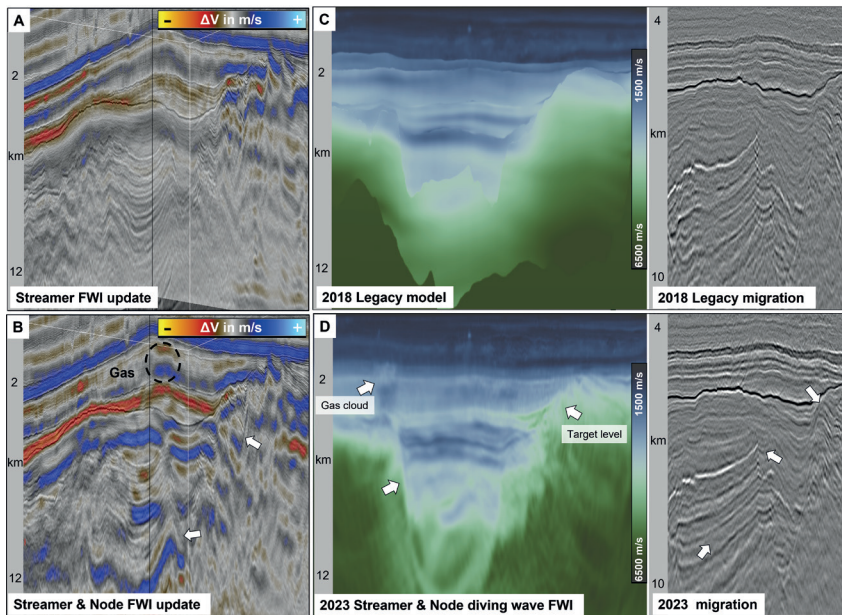


Figure 8 Oseberg survey: 3D view of streamer-only FWI perturbation in a) and diving wave node and streamer FWI perturbation in b). Legacy model and its corresponding migration in c) is compared with the 60 km-offset node and streamer FWI and its corresponding migration in d).

In comparison with the 2018 legacy model, the 6 Hz node FWI follows the sonic log more closely and, as a result, provides an improved migrated image at the target level with an uplift in fault imaging (Figure 7c).

In the Oseberg area, we addressed the presence of both shallow and deep gas anomalies using a Q-FWI and FWI-guided Q tomography to obtain a high-resolution Q model, accounting for amplitude attenuation and phase dispersion (Latter et al., 2023). This Q model was incorporated into data modelling for subsequent FWI velocity inversions, ensuring more accurate inversion convergence by reducing multi-parameter crosstalk. Even though node data were not initially used for Q-FWI, diving waves penetrating down to the deep Q anomalies enabled kinematic updates of gas reservoirs (as visible in the black circle in Figure 8b). Figure 8d illustrates the results of the 60 km-offset streamer and node diving wave FWI, effectively capturing the complexity of the velocity model across the entire survey area. This approach resolved lateral and vertical velocity variations caused by injectites, gas reservoirs in the Martin Linge and Oseberg fields, the chalk layer, heavily faulted blocks, and graben flanks, significantly improving the structural image (Figure 8d) compared to the legacy one (Figure 8c).

Elastic full-waveform inversion

North Sea geology exhibits a range of velocity anomalies and contrasts due to gas, injectites, chalk layers and the seabed. These contrasts can generate a range of elastic effects on the recorded seismic data, such as kinematic effects on pressure waves, and mode conversions between P- and S-waves. As a result, the diving-wave cone, which we usually rely on for the low-wavenumber FWI updates, may be contaminated by elastic effects (Malcolm and Trampert, 2011; Plessix and Krupovnickas, 2021). Together with other elastic effects in the wavefield, these issues can produce biased acoustic model updates for which elastic FWI is needed (Masmoudi et al., 2022; Wu et al., 2022; Zhang et al., 2023). Over the Fram and Oseberg surveys, long recorded offsets provide diving wave penetration below the sub-BCU level, which offers an opportunity to investigate the potential elastic effects around the velocity contrast at the BCU level in the Fram survey and for a shallow gas anomaly in the Oseberg survey.

For the Fram survey, we used an edited 2018 legacy model in which the sharp velocity contrast at BCU was reinforced to run both acoustic and elastic modelling. The results in Figures 9a and 9b reveal that this initial velocity model provided a better fit

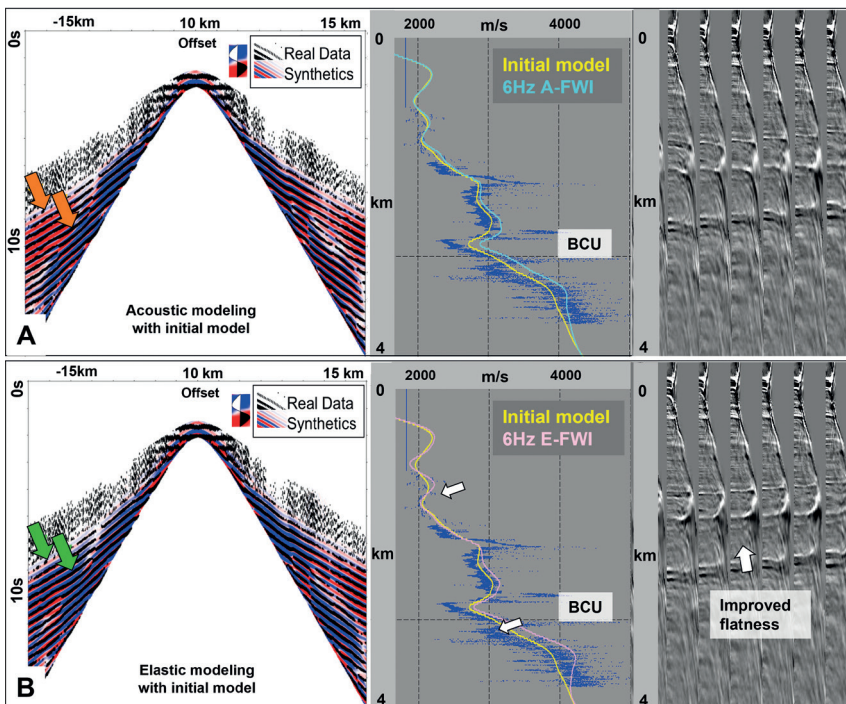


Figure 9 Fram survey: comparison of a) acoustic and b) elastic modelling using the initial velocity model. 6 Hz acoustic FWI with node data and corresponding migrated gathers (a, right) and 6 Hz elastic FWI with node data and corresponding migrated gathers (b, right).

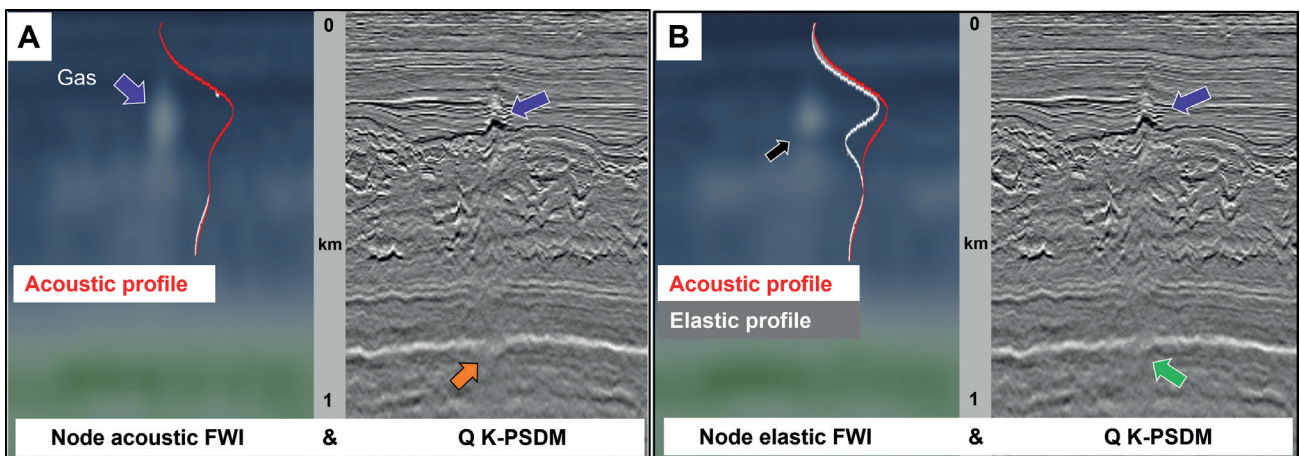


Figure 10 Oseberg survey: comparison of acoustic (a) and elastic (b) FWI results and their corresponding migrations.

between real data and synthetics generated by elastic modelling, particularly for longer offsets (over 12 km). This indicates the advantages of using elastic FWI when dealing with data acquired at such long offsets, where elastic effects are significant, and acoustic approximations fall short. Elastic FWI, although more challenging due to the need to account for V_s , was implemented by inverting for V_p using hydrophone data with a fixed V_p/V_s ratio from well logs, which is a pragmatic solution for this geological area. The acoustic and elastic inversion results (Figures 9a and 9b) demonstrate that elastic FWI with node data improves the velocity profile by enhancing the velocity contrast at the BCU level (Figure 9b, lower white arrow) and providing flatter migrated gathers compared to acoustic FWI (Figures 9a and 9b). Additionally, in the shallow section of Figure 9b (upper white arrow in the velocity profile), we observe a velocity increase recovered with elastic FWI, indicating the presence of injectite features.

In the Oseberg survey, we ran acoustic and elastic node FWI honouring the attenuation model in an area where a shallow gas

anomaly is located right above the complex injectite level. While the acoustic FWI failed to fully resolve the velocity anomaly, elastic FWI captured accurately the velocity variation induced by the gas anomaly, reducing at the same time the halo effect visible with the acoustic update (velocity profiles in Figures 10a and 10b). As a result, the distortion on the seismic image just below the gas anomaly and even deeper in the section is attenuated in the elastic case compared to the acoustic one (orange versus green arrow in Figures 10a and 10b).

High-resolution velocity model and FWI imaging

As mentioned earlier in the Nordkapp case study, one of the main requirements before considering the full wavefield in the FWI is to have an accurate and reliable long-to-mid wavelength update to which the resolution will be added. Usually, the depth of this reliable model is a function of the maximum penetration depth of the diving waves. In the Fram case, the 8 Hz diving-wave elastic FWI with node data provides an accurate and reliable update down to

the Brent level at a depth of 4 km. In the Oseberg case, the sparse node FWI provides a reliable update right down to the basement structure at a depth of 12 km. To move to the high-frequency update, a joint node and streamer FWI was run, combining all the benefits brought by each dataset: the dense spatial receiver sampling from the streamer datasets and the long-offset and full-azimuth information from the node data. The joint node and streamer FWI was run up to 30 Hz over the Fram survey and up to 40 Hz for the Oseberg survey, providing high-resolution velocity models in both cases.

Results from the Fram survey are shown in Figure 11, where we see that the 30 Hz FWI model aligns well with the sonic log down to the Brent level and effectively detects small injectite velocity contrasts (upper green arrow in Figure 11d). It

also identifies the thin limestone layer atop the target sandstone units at the BCU level (middle green arrow in Figure 11d). This high-resolution velocity model serves as a valuable attribute for geological interpretation. Below the fast limestone layer at the BCU level, the model distinguishes alternating faster and slower velocity layers within the low-velocity mudstone unit, representing shale and sandstone layers (lower green arrow in Figure 11d). Figures 11b and 11e demonstrate the seismic image improvement from the 2018 legacy model to the 30 Hz joint streamer and node FWI model. The migrated seismic image is cleaner with reduced distortion, extending from the Late Cretaceous level to the Brent (Figures 11b and 11e). Fault imaging in the tilted blocks below the BCU is also enhanced, resulting in sharper attributes as shown in Figures 11c and 11f.

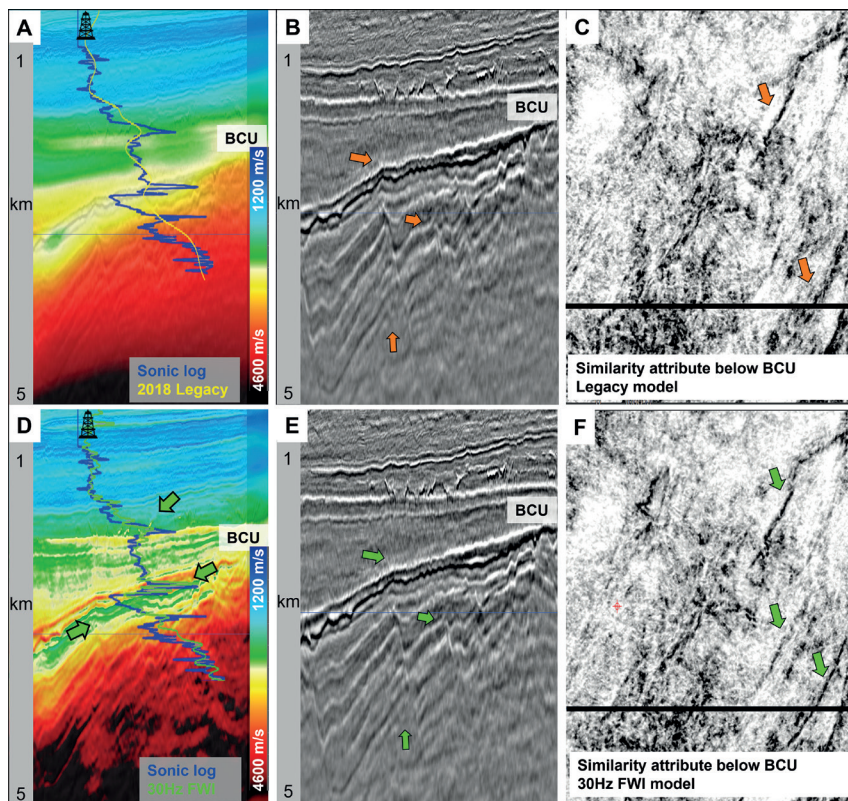


Figure 11 Fram survey: 2018 legacy model (section with velocity profile overlaid on the sonic log) in a) its migrated image in b) and the similarity attribute below BCU in c). Equivalent plots for the 30 Hz joint node and streamer FWI velocity model are shown in d), e) and f), respectively.

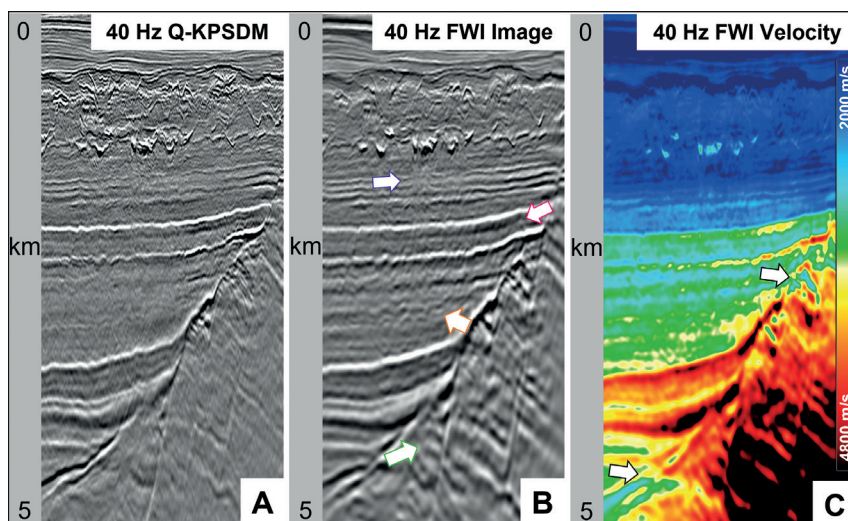


Figure 12 Oseberg survey: a) comparison of Q-KSDPM stack image filtered at 40 Hz with b) the 40 Hz FWI image. The 40 Hz FWI velocity model in c) highlights the geological complexity of the Oseberg area.

Reflectors within the faulted blocks exhibit greater continuity up to the fault planes, which are crucial for accurate prospect delineation and volumetric calculations.

Over the Oseberg survey, 40 Hz FWI was performed with the idea of directly outputting the reflectivity image to assess the benefits of FWI Imaging in exploration frontier areas, where conventional imaging suffers from limited S/N. Below the injectites level, FWI Imaging corrects for loss of illumination and for small-scale variations that induce distortion on the migrated images (purple arrow in Figure 12b). Thanks to the least-squares iteration process and full-wavefield utilisation, the FWI Image increases the S/N ratio between the Shetland and Tryggvasen levels where primary energy is weak (orange arrow in Figure 12b). Wavefront noise along the Shetland, and the BCU horizons, is attenuated on the FWI Image (pink arrow in Figure 12b). Below the BCU level, some faults are better imaged with the FWI Image and the event continuity of the sediments is improved up to the fault plane (green arrow in Figure 12b). In addition to the reflectivity, the high-resolution velocity model can be used as an interpretation attribute by highlighting potentially interesting features (white arrow in Figure 12c).

Conclusion

This paper showcases how advanced imaging techniques can be implemented to fully exploit the potential of a hybrid acquisition to address the challenge of thin reservoirs in two geologically complex regions. In the Barents Sea exploration survey covering 3700 km², FWI with node data combining active and virtual seismic helped to improve salt body delineation, overcoming streamer shortcomings. However, the node carpet sparsity ultimately prevented its usage for direct imaging or very high-frequency FWI updates. Dense streamer data remains the dataset of choice in those cases. Both data types had to work in tandem to achieve optimal velocity model building and imaging. A fully data-driven approach combining ultra-low frequencies, ultra-wide offsets and dense near offsets led to a high-resolution FWI velocity model and imaging with improved salt flank definition.

Then, in the Fram and Oseberg examples, node data provide the ultra-long offsets required to obtain a reliable low-wavenumber velocity update down to the Brent level and to capture the sharp impedance contrast and the velocity inversion below the BCU where the reservoirs lie. In addition, with long recorded offsets, the expected elastic effects induced by the large impedance contrast at this level can be observed and inverted using elastic FWI, which results in a reliable long- to mid-wavelength update down to about 5 km and 12 km depths, respectively, for the Fram and Oseberg surveys. This update subsequently unlocked the use of the full wavefield in FWI at the sub-BCU level. Full wavefields from streamer and node data were then jointly inverted up to high frequencies, producing an accurate high-resolution velocity model down to sub-BCU level. Seismic imaging and, especially, fault imaging are significantly improved with more continuous events up to the fault plane. In addition, FWI Imaging shows the benefits of high-resolution FWI for providing new insights for the interpretation and may

unlock new targets in unexplored areas of the deeper part of the sedimentary basin.

This innovative acquisition design enables the application of advanced subsurface imaging technologies such as interferometry and elastic FWI down to reservoir depths. It holds promise for near-field exploration and broader basin exploration. Depending on prospect depths, transitioning to a denser node grid, from 1 km to 500 m spacing, could be considered to harness node data for higher frequencies and refined FWI Images.

Acknowledgements

We thank CGG Earth Data, AkerBP and its partners DNO Norge AS and Petoro AS in PL1083, for permission to publish this work. We also thank our colleagues Olivier Leblanc and Mathieu Reinier for fruitful discussions on new imaging technologies and Jaswinder Mann-Kalil and Gustav Aagenes Ersdal for their geological insights.

References

- Bardainne, T. [2018]. *Joint inversion of refracted P-waves, surface waves and reflectivity*. 80th EAGE Annual Conference & Exhibition, Extended Abstracts, We K 02.
- Dellinger, J., Brenders, A.J., Sandschaper, J.R., Regone, C., Etgen, J., Ahmed, I. and Lee, K.J. [2017]. *The Garden Banks model experience*. *The Leading Edge*, **36**(2), 151-158.
- Dhelie, P.E., Danielsen, V. and Lie, J.E. [2021]. Combining nodes and streamers to tackle the imaging challenges of salt basins in the Barents Sea. First International Meeting for Applied Geoscience & Energy, *SEG Technical Program Expanded Abstracts*, 41-45.
- Henin, G., Espin, I., Salaun, N., Masclet, S., Dhelie, P.E., Danielsen, V. and Lie, J.E. [2022]. Large-Scale 3D High-Resolution Near-Surface Imaging over Nordkapp. 83rd EAGE Annual Conference & Exhibition, *Extended Abstracts*, 1-5.
- Latter, T., Nielsen, K.M., Beech, A. and Cantu Bendeck, D. [2023]. Deriving a high-resolution regional scale Q model over the Northern Viking Graben. *84th EAGE Annual Conference & Exhibition, Extended Abstracts*, 1-5.
- Le Meur, D., Solyga, D., Prescott, A., Courbin, J. and Donno, D. [2020]. Retrieving ultra-low frequency surface waves from land blended continuous recording data. *SEG Technical Program Expanded Abstracts*, 1855-1859.
- Lie, J.E., Danielsen, V., Dhelie, P.E., Sablon, R., Siliqi, R., Grubb, C., Vinje, V., Nilsen, C. and Soubaras, R. [2018]. *A Novel Source-Over-Cable Solution to Address The Barents Sea Imaging Challenges*. Marine Acquisition Workshop, EAGE, cp-560-00016.
- Lie, J.E., Vettle, V., Dhelie, P.E., Jiang, H., Danielsen, V. and Salaun, N. [2022]. Nordkapp Topseis/Node Acquisition—Lessons from a Modelling Study. *First Break*, **40**(2), 41-49.
- Long, A. [2017]. Source and streamer towing strategies for improved efficiency, spatial sampling and near offset coverage. *First Break*, **35**(11), 71-74.
- Malcolm, A.E. and Trampert, J. [2011]. Tomographic errors from wave front healing: More than just a fast bias. *Geophysical Journal International*, **185**(1), 385-402.
- Masmoudi, N., Stone, W., Ratcliffe, A., Refaat, R. and Leblanc, O. [2022]. Elastic Full-Waveform Inversion for Improved Salt Model

- Building in the Central North Sea. *83th EAGE Annual Conference & Exhibition, Workshop Programme, Extended Abstracts*, 1-3.
- Michell, S., Shen, X., Brenders, A., Dellinger, J., Ahmed, I. and Fu, K. [2017]. Automatic velocity model building with complex salt: Can computers finally do an interpreter's job? *87th Annual International Meeting, SEG, Expanded Abstracts*, 5250-5254.
- Plessix, R.-E., and Krupovnickas, T. [2021]. Low-frequency, long-offset elastic waveform inversion in the context of velocity model building. *The Leading Edge*, **40**(5), 342-347.
- Shen, X., Ahmed, I., Brenders, A., Dellinger, J., Etgen, J., and Michell, S. [2017]. Salt model building at Atlantis with Full Waveform Inversion. *87th Annual International Meeting, SEG, Expanded Abstracts*, 1507-1511.
- Strobbia C., Laake, A., Vermmer, P. and Glushchenko, A. [2011]. Surface waves: use them then lose them. Surface wave analysis, inversion, and attenuation in land reflection seismic surveying. *Near-surface Geophysics*, **9**(6), 503-513.
- Wu, Z., Wei, Z., Zhang, Z., Mei, J., Huang, R. and Wang, P. [2022]. Elastic FWI for large impedance contrasts. *Second International Meeting for Applied Geoscience & Energy, SEG/AAPG, Expanded Abstracts*, 3686-3690.
- Xiao, B., Ratcliffe, A., Latter, T., Xie, Y. and Wang, M. [2018]. Inverting near-surface absorption bodies with full-waveform inversion: a case study from the North Viking Graben in the Northern North Sea. *80th EAGE Conference & Exhibition, Extended Abstracts*, Tu A12 03.
- Zhang, Z., Mei, J., Lin, F., Huang, R. and Wang, P. [2018]. Correcting for salt misinterpretation with full-waveform inversion. *88th Annual International Meeting, SEG, Expanded Abstracts*, 1143-1147.
- Zhang, Z., Wu, Z., Wei, Z., Mei, J., Huang, R. and Wang, P. [2020]. FWI Imaging: Full-wavefield imaging through full-waveform inversion. *90th Annual International Meeting, SEG, Expanded Abstracts*, 656-660.
- Zhang, Z., Wu, Z., Wei, Z., Mei, J., Huang, R. and Wang, P. [2023]. Enhancing salt model resolution and subsalt imaging with elastic FWI. *The Leading Edge*, **42**(3), 207-215.

ADVERTISEMENT



Publish with EAGE



To serve the interests of our members and the wider multidisciplinary geoscience and engineering community, EAGE publishes a range of books and scientific journals in-house. Our extensive, professional marketing network is used to ensure publications get the attention they deserve.

EAGE is continually seeking submissions for both book publishing and articles for our journals.

A dedicated and qualified publishing team is available to support your publication at EAGE.

CONTACT OUR PUBLICATIONS DEPARTMENT AT PUBLICATIONS@EAGE.ORG!